Research Paper

PAIN 00 (2026) 1–13

PAIN®

VIDEO

Male-specific analgesic effects of minocycline in sickle cell disease are mediated by microglia and the microbiome

Juanna M. John, Zulmary Manjarres, Nurfatihah I. Zulkifly, Ashley N. Plumb, McKenna L. Pratt, Katelyn E. Sadler*

Abstract

Over 50% of individuals with sickle cell disease (SCD) experience chronic pain that is phenotypically distinct from their acute, vaso-occlusive crisis pain. Chronic SCD pain is commonly managed with opioid-based drugs that are associated with unwanted side effects, incomplete pain relief, and—in this population—accessibility issues. Thus, new treatments for chronic SCD pain are desperately needed. Here, we examined the analgesic efficacy of acute minocycline treatment in transgenic SCD mice. Sickle cell disease mice exhibit gut dysbiosis and chronic inflammation. Therefore, we hypothesized that minocycline would provide robust analgesia in this model given the drug's antibiotic and anti-inflammatory properties, respectively. Six days of minocycline treatment reversed chronic mechanical hypersensitivity only in male SCD mice. We identified 2 potential mechanisms underlying these sex-specific effects. First, we observed increased microgliosis only in the dorsal horn of male SCD mice. Minocycline treatment had opposite effects on microglial number in male and female SCD spinal cords. Second, minocycline treatment altered the gut microbiota in a sex-specific fashion; fecal microbiota transplant (FMT) from minocycline-treated female SCD mice induced widespread pain in recipients, whereas FMT from minocycline-treated male SCD mice did not. In summary, these experiments highlight novel sex-specific mechanisms of minocycline analgesia and support future exploration of minocycline use for SCD pain management, but only in male patients.

Keywords: sickle cell, microbiome, microglia, minocycline, sex differences

1. Introduction

Chronic pain is a debilitating symptom experienced by individuals with sickle cell disease (SCD).[11] Worldwide, approximately 7.74 million individuals suffer from this genetic blood disorder,[70] which—in addition to pain—is characterized by hemolytic anemia, chronic inflammation,[15] and changes in the gut microbiome.[4,8,9,19,21,40,49] Individuals with SCD describe their chronic pain as phenotypically distinct from the pain they experience during an acute vaso-occlusive episode.[17,25] Verbal descriptions of chronic SCD pain include words that suggest both nociceptive (eg, throbbing, piercing, crushing) and neuropathic (eg, aching, shooting, stabbing) underlying mechanisms.[6,29] As such, the most successful analgesic strategies for alleviating chronic SCD pain are likely to be those that target multiple pathological processes. Current guidelines for pharmacological management of chronic SCD pain include use of nonsteroidal anti-inflammatory drugs (NSAIDs), serotonin and norepinephrine reuptake inhibitors, tricyclic antidepressants, and gabapentinoids.[5] Unfortunately, these drugs and opioid-based therapies, which have additional unwanted side effects, often fail to completely alleviate chronic SCD pain. Thus, additional drug classes with multiple modes of analgesic action should be considered for use in individuals with SCD.

Chronic inflammation and gut dysbiosis are 2 hallmarks of SCD that contribute to chronic pain and likely develop as a result of disease-associated hemolysis and vaso-occlusion.[15] Upon sickling, erythrocytes in both patients and mice with SCD release proinflammatory compounds (eg, reactive oxygen species), adhere to the vascular endothelium and circulating immune cells, and ultimately, undergo hemolysis, which results in the elevation of circulating damage associated molecular patterns (DAMPs; eg, heme, ATP). These red cell–derived DAMPs can activate microglia—resident immune cells of the central nervous system (CNS) that are increased in both number and activation status in the SCD mouse spinal cord dorsal horn.[71] In addition, work from our own laboratory recently demonstrated that hemolysis-associated metabolites in the gastrointestinal tract alter the gut microbiota and drive chronic pain in SCD mice.[4] Until curative SCD therapies become widely available and erythrocyte sickling can be prevented from the time of birth, analgesic therapies that simultaneously alter the gut microbiome and limit inflammation may provide significant relief for those suffering from SCD pain.

To this end, we examined the analgesic efficacy of minocycline in SCD mice. Minocycline is an inexpensive, widely available drug that was originally characterized as a broad spectrum tetracycline

Sponsorships or competing interests that may be relevant to content are disclosed at the end of this article.

Department of Neuroscience, Center for Advanced Pain Studies, University of Texas at Dallas, Richardson, TX, United States

**Corresponding author. Address: Department of Neuroscience, Center for Advanced Pain Studies, University of Texas at Dallas, 800 W Campbell Rd, Richardson, TX 75080, United States. Tel.: (972) 883-2406. E-mail address: katelyn.sadler@utdallas.edu (K. E. Sadler).*

Supplemental digital content is available for this article. Direct URL citations appear in the printed text and are provided in the HTML and PDF versions of this article on the journal's Web site (www.painjournalonline.com).

http://dx.doi.org/10.1097/j.pain.0000000000004008

antibiotic.[54,61] Tetracyclines limit bacterial growth by binding to the 30S bacterial ribosome subunit, thus inhibiting protein translation. Minocycline activity is not limited to prokaryotic cells, however; minocycline modulation of host immune cell function also limits inflammation and pain in a variety of clinical conditions and rodent models.[46,55] In these studies, we administered minocycline to male and female SCD mice for 6 days and then assessed pain-like behaviors, changes in the gut microbiota composition, and microglial activation in the spinal cord dorsal horn—a key relay in CNS nociceptive networks. Our goal for this study was not only to assess the analgesic efficacy of minocycline in SCD but to further understand the cellular basis—both prokaryotic and eukaryotic—of chronic pain in SCD.

2. Methods

2.1. Mice

These experiments primarily used the Townes mouse model of SCD.[76] In this model, endogenous murine α- and β-globin genes are knocked out and replaced with human γ-, α-, and either normal ("A") or sickle ("S") β-globin genes. Mice homozygous for sickle β-globin (HbSS) display many SCD characteristics including sickled erythrocytes, hemolytic anemia,[76] hypoxia-reoxygenation–inducible acute pain,[10] spontaneous chronic pain,[56,63] and persistent hypersensitivity to mechanical and cold stimuli.[35,43,66,82] Mice homozygous for wildtype β-globin (HbAA) are used as controls. All mice were genotyped at the time of weaning using standard PCR protocol provided on The Jackson Laboratory Web site (strain #013071). Male and female HbAA and HbSS mice aged 6 to 11 months were used in experiments. We elected to use older animals in these studies given that the chronic pain phenotype is more severe in aged (>6 months) Townes HbSS mice.[47,82] C57BL/6J male and female mice, aged 8 to 12 weeks, were used as fecal material transplant recipients. All mice were bred in-house and had ad libitum access to food and water throughout the duration of all experiments. Mice were randomized to treatment groups. All animal experiments and procedures in this study were done after approval from the Institutional Animal Care and Use Committee of the University of Texas at Dallas (protocol #2022-0088).

2.2. Pain-like behavioral assays

Experimenters were blinded to mouse genotype and/or treatment group during behavioral testing and analysis. All testing was completed in Plexiglass behavior chambers (10 × 10 × 20 cm); chambers were placed on a raised wire mesh grid for mechanical assays and a 1/4' thick piece of glass for dry ice testing. Animals were habituated to the testing environment for at least 1 hour before testing. The experimenter was present for at least the last 30 minutes of this habituation period.

2.2.1. Von Frey mechanical hypersensitivity testing

The up-down von Frey assay was used to measure punctate mechanical hypersensitivity as previously described.[13] Hind paw 50% withdrawal thresholds were recorded by applying calibrated von Frey filaments (0.02-2.56 g) at a 30° angle to the center of the plantar surface of each hind paw for 2 seconds. If the mouse raised its stimulated paw from the mesh, it was classified as a response. If the first filament elicited a withdrawal, the next lower force filament was then used to stimulate the same paw. Conversely, if a withdrawal was not detected with the first filament, the next larger force filament was used. After the first series of opposite reactions (ie, withdrawal response followed by no response or vice versa), each hind paw was stimulated 4 more times. The 50% withdrawal threshold for each hind paw was separately calculated as described[22] before being averaged for each animal.

2.2.2. Needle mechanical hyperalgesia testing

Hind paw needle stimulation was used to measure mechanical hyperalgesia as previously outlined.[36] Needle responses were elicited by poking the center of the plantar surface of each hind paw with a 27Ga spinal needle. Subsequent responses were classified into 3 categories: null, normal, and nocifensive. Null responses were those in which the animal did not respond to stimulation. Normal responses were those in which the animal lifted then returned its paw to the wire mesh. Responses were classified as nocifensive when the animal raised its paw and additionally shook, licked, or persistently elevated the paw. Needle testing was repeated 5 times on each paw, and then response frequency and types were summed between paws.

2.2.3. Brush dynamic mechanical allodynia testing

Hind paw brush stimulation was used to measure dynamic mechanical allodynia as previously described.[16] Brush responses were elicited by lightly dragging a 10/0 short liner paintbrush across the entire glabrous surface of each hind paw from heel to toe. Responses to dynamic brush stimulation were characterized and analyzed like the needle assessment.

2.2.4. Plantar dry ice cold hypersensitivity testing

The plantar dry ice assay measured hypersensitivity to cold stimulation as previously described.[7] Dry ice was crushed into a powder, loaded into a plastic applicator, and then applied to the glass directly below each hind paw; the time taken to withdraw each paw (withdrawal latency; not to exceed 20 seconds) was recorded. The withdrawal latency was measured 5 times for each paw and then averaged between paws to calculate the overall withdrawal latency for a single mouse.

2.3. Animal treatments

2.3.1. Minocycline administration

Townes HbAA and HbSS mice had ad libitum access to 100 mg/kg minocycline treatment (Santa Cruz Biotechnology, Dallas, TX, USA Cat# sc-203339B) for 6 days; similar doses of minocycline have previously been shown to decrease immune cell infiltration in the HbSS CNS.[20] Water bottles were weighed and refilled every other day. Pain-like behavior tests were performed before and after 6 days of vehicle (water) or minocycline treatment.

2.3.2. Fecal microbiota transplant paradigm

Fecal material was collected immediately upon defecation from vehicle- or minocycline-treated (days 4-10 of treatment) HbAA and HbSS mice. Fecal donors were housed in 2 separate cages to limit cage effects frequently observed in microbiome studies. Upon defecation, feces were frozen at −80°C or immediately homogenized in vivarium drinking water (1 pellet/1 mL water). Homogenized fecal material was administered to naïve, sex-

matched C57BL/6 mice every other day for 7 days (4 fecal microbiota transplant [FMTs] total; 200 μL p.o.). Pain-like behavior assessments were performed before FMT (B: baseline), on the day between the third and fourth FMTs (FMT), and 7 and 14 days after the final FMT.

2.4. Gross anatomical assessments

One day after the completion of behavior testing, animals were euthanized via sodium pentobarbital injection. Tissues/samples of interest (spleen, small intestine, colon, cecum, fecal material, and spinal cord) were collected and processed as described below. The spleen and cecum were removed and immediately weighed. The small intestine and colon were removed, cleaned of residual mesentery, and measured for length. Fecal samples and spinal cord collection methods are outlined below.

2.5. Spinal cord Iba1+ immunofluorescent staining

2.5.1. Spinal cord tissue processing

After mice were euthanized, spinal cords were dissected and drop fixed in 4% paraformaldehyde (PFA) overnight at 4°C. Spinal cords were cryopreserved in 30% sucrose at 4°C for 48 hours and then embedded in optimal cutting temperature media before being sectioned on a cryostat. Tissue was sliced transversally at 30 μm and stored in 1X phosphate buffered saline (PBS; 4°C) before staining.

2.5.2. Iba1 immunofluorescent staining

Sections (6 per animal) containing lumbar spinal cord (L4-L6) were mounted onto SuperFrost Plus slides and then incubated in blocking solution (3% normal goat serum, 2% bovine serum albumin, 1% Triton-X100, 0.05% Tween-20, and 1X PBS) for 1 hour. Spinal cord sections were immunostained with a rabbit anti-Iba1 (1:500; Wako Fujifilm, Santa Ana, CA, USA, Cat# 019-19741). After washing several times, sections were incubated with a AlexaFluor-488 goat ant-irabbit IgG (H + L) (1:500, Invitrogen, Carlsbad, CA, USA, Cat#: A11008) and Hoechst 33342 (1:1000, Invitrogen, Cat# H3570). All sections were mounted with ProLong Gold antifade reagent.

2.5.3. Confocal imaging and analysis of microglia

For analysis of Iba1, 3 images of either left or right dorsal horn were collected at 20X per animal using a FV-4000 (Olympus, Tokyo, Japan; UPlanXApo 20X/0.80/0.17/OFN26.5) confocal microscope. Note, no differences in Iba1 staining were observed between left and right dorsal horn within a given animal. Images were digitized with confocal Z-stacks, and maximum intensity projection was analyzed. The number of Iba1+ cells in laminae I, II, and III was counted manually using the cell counter plugin in Image J (http://imagej.nih.gov). The investigator was blinded to treatment and genotype during cell counting.

2.5.3.1. Morphometric feature extraction

Microglial morphology was quantified from image-derived outputs generated using the MicrogliaMorphology ImageJ pipeline (FracLac and skeletonization outputs).[42] MicrogliaMorphology is an ImageJ macro that integrates the following ImageJ plugins: including *Analyze Particles*, *Skeletonize (2D/3D)*, and *Analyze-Skeleton*. Two independent feature tables—one derived from FracLac and one from skeleton-based analyses—were imported and merged at the single-cell level. Each row corresponded to an individual segmented microglial cell, and columns represented morphometric measurements capturing fractal properties and skeleton-based branching descriptors. Experimental metadata embedded in file names were parsed into explicit columns using a fixed separator. Metadata included animal identifier (ID), sex, genotype, treatment, spinal level, and antibody. This ensured that all downstream analyses were performed using explicitly defined experimental factors rather than string-matched file names.

2.5.3.2. Feature correlation analysis

To assess redundancy among morphometric features and characterize relationships between related descriptors, pairwise correlations were computed across 27 morphometric features. Correlation heatmaps were generated using user-defined correlation and significance thresholds, and the underlying correlation coefficients and *P*-values were extracted. This analysis was used to confirm expected clustering of related measures (eg, branching complexity metrics) and to inform interpretation of multivariate structure, rather than to exclude features automatically.

2.5.3.3. Principal component analysis of morphometric features

Morphometric features were log-transformed before dimensionality reduction. Principal component analysis (PCA) was performed over the selected feature range using helper functions from MicrogliaMorphologyR.[42] The number of retained principal components (PCs) was guided by an elbow-style diagnostic. Principal component scores were exported for downstream analyses. To aid interpretation of PC axes, correlations between PCs and original morphometric features were computed and visualized, identifying features that loaded most strongly onto each PC.

2.5.3.4. Construction of clustering input

To classify individual microglia into morphological classes, the pipeline standardized (z-scored) the first 3 principal components (PC1-PC3), which together explained approximately 87% of the total variance. These scaled PCs were used as the clustering input space, reducing noise and collinearity relative to clustering in the raw feature space.

2.5.3.5. Cluster number selection and clustering

The number of clusters was evaluated using within-cluster sum-of-squares and silhouette diagnostics applied to a random subsample of cells (n = 1000) to reduce computational burden. Both metrics supported a four-cluster solution as optimal. Final cell assignments were obtained using hard k-means clustering (k = 4). Cluster identities were appended to the PCA scores and raw-feature tables, enabling visualization of clusters in PC space and examination of cluster-specific feature distributions.

2.5.3.6. Cluster characterization and animal-level cluster composition

Numeric cluster labels were mapped to biologically interpretable morphological phenotypes (Rod-like, Ameboid, Ramified, Hypertrophic) based on cluster-specific feature profiles. Cluster composition was quantified as the percentage of cells belonging to each cluster within each animal and experimental condition. Percentages were computed per animal and grouped by cluster, sex, genotype, treatment, and antibody. Treatment order (vehicle, minocycline) was fixed to ensure consistent plotting and interpretation.

2.5.3.7. Cluster proportion analyses by sex and treatment

Downstream inferential analyses were restricted to HbSS genotype (SCD) animals and Iba1 positive cells. Cluster labels were standardized and coerced to factors with a fixed biologically meaningful order. To ensure that each animal contributed a single observation per cluster within each sex and treatment, cluster percentages were averaged within animal when repeated entries existed (eg, across all L5 spinal levels). To compare cluster proportions across morphological classes within sex × genotype panels and within each treatment, nonparametric pairwise Wilcoxon tests were performed with Benjamini–Hochberg false discovery rate (FDR) correction. Adjusted *P*-values were formatted and annotated on plots using *ggpubr* utilities.

2.5.3.8. Sex-dependent effects and effect size estimation

For each cluster within each treatment, sex differences in cluster proportions were tested using the Wilcoxon rank-sum (Mann–Whitney) test with Benjamini–Hochberg correction across clusters and treatments. Effect sizes were quantified using Cliff delta, a nonparametric measure of stochastic dominance that provides both direction and magnitude of group differences and is robust to non-normal distributions and unequal variances. For targeted clusters (eg, ramified and rod-like), Cliff delta was computed and annotated directly on the figures alongside adjusted *P*-values.

2.5.3.9. Morphometric feature-level sex effects and multivariate importance

Morphometric features were reshaped into long format, and Cliff delta was computed for each treatment × feature combination to quantify sex-dependent effects. The pipeline implements explicit checks for missing sex levels and returns NA when comparisons are not valid. Separately, treatment-specific partial least squares discriminant analysis (PLS-DA) models were fitted using sex as the response variable. Variable importance in projection (VIP) scores were extracted from each model (mixOmics package) and averaged across components up to the selected number of components to yield a single importance score per feature. Variable importance in projection scores and Cliff delta estimates were joined by treatment and feature. Features were classified as integrated "hits" based on joint thresholds for multivariate importance and effect magnitude (eg, VIP $\geq$ 1.0 and $|\delta| \geq 0.33$). Scatter plots of VIP vs Cliff delta were generated per treatment, with threshold lines indicating selection criteria and point aesthetics reflecting hit status and sex bias direction.

2.5.3.10. Cluster phenotype partial least squares discriminant analysis and effect size visualization

In addition to morphometric feature–based analyses, a compact PLS-DA was performed using the 4 cluster percentages as predictors and sex as the response variable, separately within each treatment. Variable importance in projection scores was extracted per cluster to quantify their contribution to sex discrimination. Cliff delta was computed for each cluster within each treatment using the same phenotype matrix, providing direction and magnitude of sex bias in cluster composition. Rather than displaying composite scores as horizontal bar plots, treatment effects within each sex were summarized using a forest plot representation. In this visualization, Cliff delta estimates (minocycline vs vehicle) were plotted for each cluster, stratified by sex, with a vertical reference line at zero indicating no treatment effect.

2.5.3.11. Quality control and reproducibility

Partial least squares discriminant analysis models included explicit checks for minimum sample size and class balance within each treatment and sex stratum. Models failing these criteria were skipped to avoid unstable inference. All analyses were conducted in R using fixed random seeds to ensure reproducibility. Source code for MicrogliaMorphologyR and detailed function descriptions are available at https://github.com/zulmarymanjarresfarias02/MicrogliaMorphology-outputs-minocycline-paper-/tree/main.

2.6. Fecal bacterial DNA analysis

2.6.1. Feces collection

Fecal material for quantitative real-time PCR (qRT-PCR) analysis was collected by cutting longitudinally through the colon. Fresh fecal material was removed from the colon and then immediately placed into empty microcentrifuge tubes on dry ice. Feces were stored at −80°C until extraction.

2.6.2. Fecal DNA extraction

Fecal DNA extraction was performed using a modified version of the Qiagen PowerLyzer Power Soil Kit as previously reported.[44] Fecal material was added to a PowerBead tube for every animal. DNA was then extracted from the fecal material in line with previous reports. DNA concentration was measured using a NanoDrop, and for analysis purposes, normalized to starting fecal mass.

2.6.3. Quantitative real-time PCR of bacterial phyla

Quantitative real-time PCR was completed using phylum-specific and universal bacterial 16S rRNA gene primers (**Table 1**). 10 ng of template DNA was run in triplicate for each sample and primer set. Amplification was monitored in real-time via PowerUp SYBR Green fluorescence signal and the following 3-step protocol: 40 cycles of 10 seconds at 95°C, 10 seconds at 60°C, and 30 seconds at 72°C. The ΔCt method was used to compare across phyla changes between sexes and treatment groups; the ΔΔCt method was used to analyze within phyla changes between sexes and treatment groups.

2.7. Statistics

All data were analyzed using GraphPad Prism 10. Results were considered statistically significant when $P < 0.05$. Results from von Frey tests, dry ice testing, anatomical measures, qPCR, and metabolomics were analyzed with 1-, 2-, or 3-way ANOVA depending on the number of independent variables. If a significant main effect was observed in the ANOVA, Bonferroni post-hoc comparisons were completed. Microglial staining was analyzed with unpaired *t* tests. Needle and paintbrush behaviors were analyzed via χ^2 analyses and Fisher post-hoc tests.

3. Results

3.1. Short-term minocycline administration reduces chronic pain in male, but not female, sickle cell disease mice

To determine the analgesic efficacy of minocycline in chronic SCD pain, pain-like behavior testing was completed in male and female SCD mice (HbSS) and hemoglobin control mice (HbAA)

Table 1

Quantitative real-time PCR bacterial primers.

Gene target	Forward primer	Reverse primer	Reference
16S rRNA	ACT CCT ACG GGA GGC AGC AG	TTA CCG CGG CTG CTG GCA C	Huse et al.[37]
Bacteroidetes	GTT TAA TTC GAT GAT ACG CGA G	TTA ASC CGA CAC CTC ACG G	Yang et al.[81]
Firmicutes	GGA GYA TGT GGT TTA ATT CGA AGC A	AGC TGA CGA CAA CCA TGC AC	Guo et al.[32]
Actinobacteria	TGT AGC GGT GGA ATG CGC	AAT TAA GCC ACA TGC TCC GCT	Yang et al.[81]
Verrucomicrobia	TCA KGT CAG TAT GGC CCT TAT	CAG TTT TYA GGA TTT CCT CCG CC	Yang et al.[81]

after 6 days of minocycline treatment. Minocycline treatment effectively alleviated punctate mechanical allodynia (**Fig. 1A**), dynamic mechanical allodynia (**Fig. 1B**), and mechanical hyperalgesia (**Fig. 1C**) in male SCD mice but had no effect on cold hypersensitivity (**Fig. 1D**). Very different observations were made in female mice. Unlike in male counterparts, minocycline treatment failed to reverse mechanical allodynia (**Figs. 1E and F**) or mechanical hyperalgesia (**Fig. 1G**) in female SCD mice; cold hypersensitivity was not observed in this cohort of SCD female mice despite our previous reports clearly demonstrating this phenotype (**Fig. 1H**).[65,66] Thus, the analgesic efficacy of short-term minocycline treatment in SCD is specific to males.

3.2. Minocycline administration has sex-specific effects on pathological organs in sickle cell disease mice

We next wanted to determine the manner in which minocycline induced sex-specific analgesia. To begin this analysis, gross anatomical observations were collected for organ systems associated with SCD pathology and pain. Minocycline treatment did not induce significant changes in male mouse body weight (**Fig. 2A**), but it significantly decreased splenomegaly (**Fig. 2B**), a signature of the Townes SCD transgenic mouse model.[3] Increased spleen size in SCD mice may result from accumulation of sickled erythrocytes, bone marrow–independent hematopoiesis, and heightened immune surveillance, particularly of microbial pathogens. Thus, smaller spleen size in minocycline-treated SCD mice may result from a change in gut bacterial populations and resulting immune responses. Minocycline did not affect additional organs of interest in male SCD mice; small intestine and colon length did not differ between genotypes or treatment groups (**Figs. 2C and D**).

The effects of minocycline on female SCD organ systems differed from those observed in males. Minocycline did not change body mass (**Fig. 2E**), relative spleen size (**Fig. 2F**), or small intestine length of female SCD mice (**Fig. 2G**). However, different from male counterparts, female SCD mice had shorter colons than female control mice, a phenotype that was reversed after 1 week of minocycline treatment (**Fig. 2H**). Colonic shortening is observed in rodent models of intestinal inflammation.[28] Thus, although minocycline treatment does not alleviate

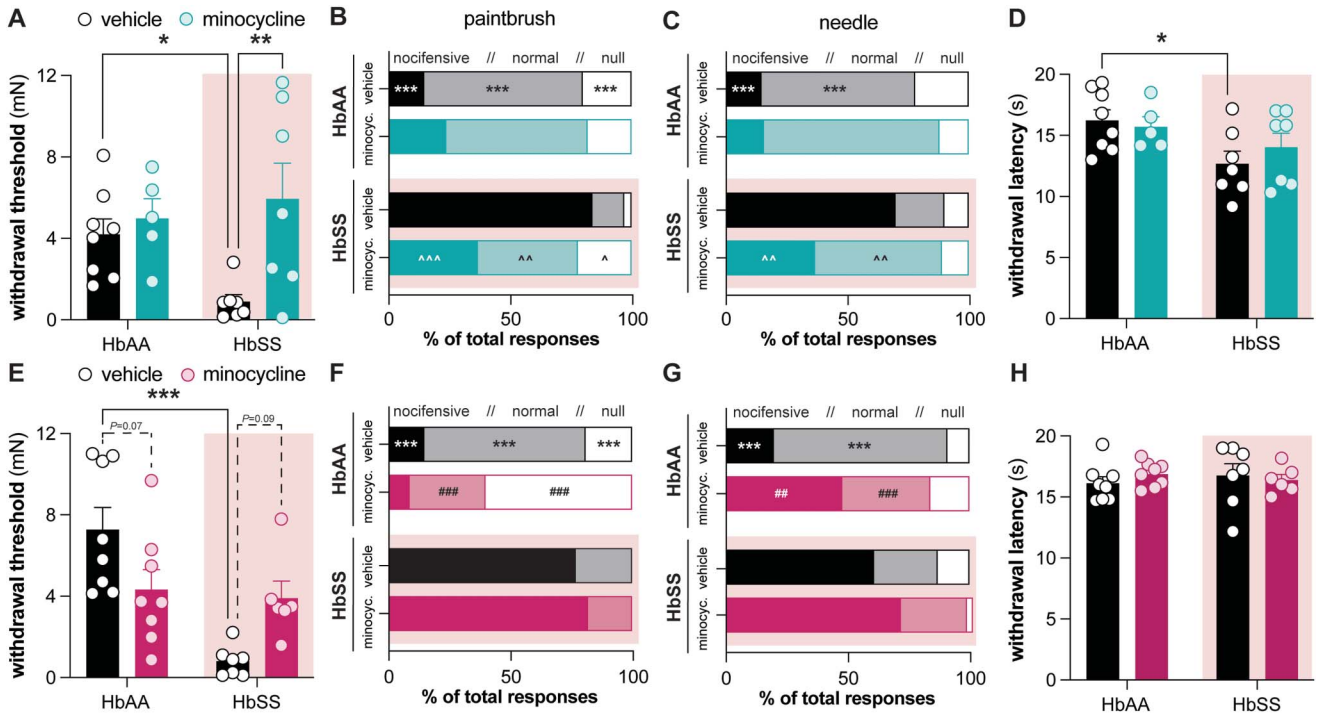

Figure 1. Minocycline alleviates chronic mechanical hypersensitivity in male SCD mice but not in female SCD mice. Male (teal) and female (magenta) SCD mice were maintained on *ad libidum* minocycline treatment (100 mg/kg) for 6 days. Hind paw (A) mechanical withdrawal thresholds, (B) sensitivity to dynamic paintbrush stimulation, (C) sensitivity to noxious needle stimulation, and (D) sensitivity to noxious cold stimulation of male mice on day 6 of vehicle or minocycline treatment. Hind paw (E) mechanical withdrawal thresholds, (F) sensitivity to dynamic paintbrush stimulation, (G) sensitivity to noxious needle stimulation, and (H) sensitivity to noxious cold stimulation of female mice on day 6 of vehicle or minocycline treatment. $N=5$ to 8 mice per group; panels (B, C, F, G): *vehicle HbAA vs HbSS, #HbAA vehicle vs minocycline, ^HbSS vehicle vs minocycline. HbAA, homozygous for wildtype β-globin; HbSS, homozygous for sickle β-globin; SCD, sickle cell disease.

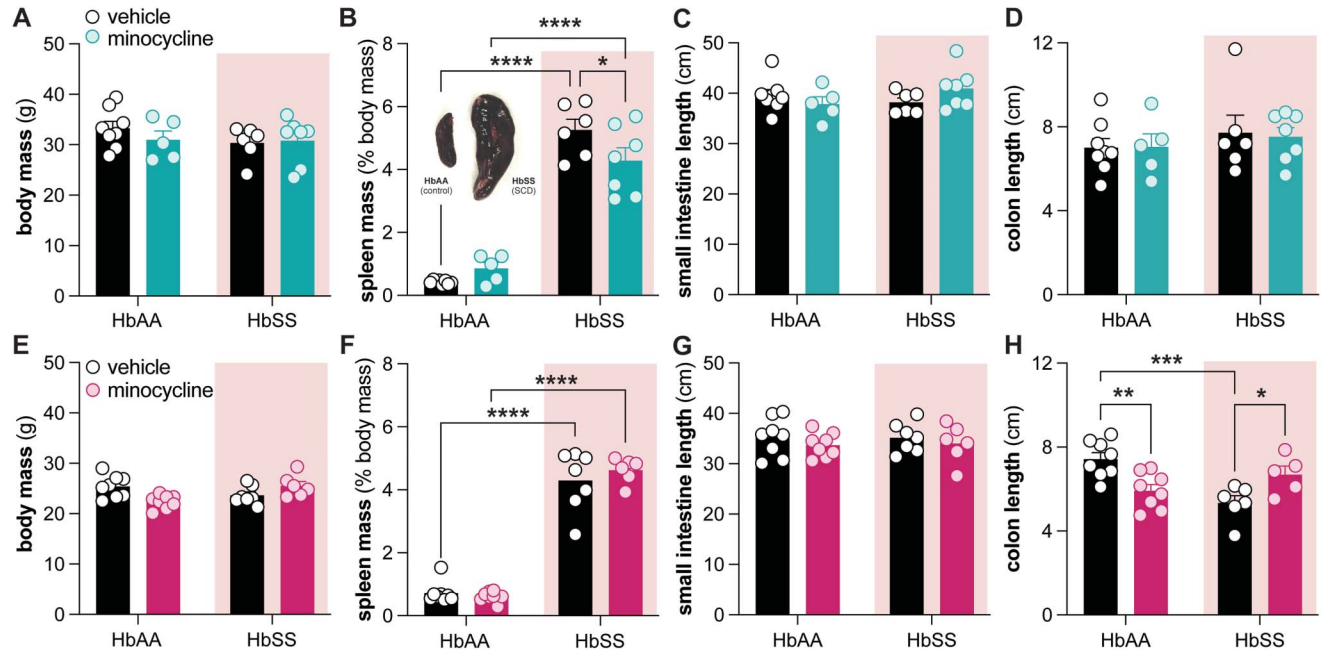

Figure 2. Differential effects of minocycline on gross inflammatory indicators in SCD mice. Male (teal) and female (magenta) SCD (HbSS) and hemoglobin control (HbAA) mice were maintained on *ad libidum* minocycline treatment (100 mg/kg) for 6 days. Gross anatomical observations recorded from male mice on day 6 of treatment included (A) body mass, (B) relative spleen mass, (C) small intestine length, and (D) colon length. Measures recorded from female mice on day 6 of treatment were identical to those recorded in males and included (E) body mass, (F) relative spleen mass, (G) small intestine length, and (H) colon length. Bonferroni post-hoc tests: $^{*}P < 0.05$, $^{**}P < 0.01$, $^{***}P < 0.001$, $^{****}P < 0.0001$. HbAA, homozygous for wildtype β-globin; HbSS, homozygous for sickle β-globin; SCD, sickle cell disease.

reflexive pain measures in female SCD mice, it may still decrease colonic inflammation in a sex-specific manner.

3.3. Minocycline analgesia in male sickle cell disease mice results, in part, from altered microglia number and morphology in spinal cord

Historically, minocycline analgesia is primarily attributed to its anti-inflammatory properties, most notable of which is its ability to suppress microglia activation in the central nervous system.[27] Intriguingly, functional consequences of this microglial suppression can be sexually dimorphic; despite exhibiting similar levels of injury-induced microgliosis, minocycline treatment induces sex-specific changes in microglial gene expression and metabolite release after injury.[2,23,69] Given this, we hypothesized that the sex-specific analgesic effects of minocycline treatment may result from differential effects on microglial activity in central nociceptive circuits. To assess this possibility, Iba1 immunostaining was performed on lumbar spinal cord isolated from vehicle- and minocycline-treated SCD mice (**Figs. 3A, C, E**). More microglia were observed in the dorsal horn of vehicle-treated male SCD mice as compared to vehicle-treated female SCD mice (**Fig. 3B**). Furthermore, minocycline treatment had opposing effects on microglial number in male and female mice; minocycline treatment trended to decrease microglial number in male SCD mice (**Fig. 3D**) while increasing microglial number in female mice (**Fig. 3F**; 2-way ANOVA of data from 3D and 3F combined: overall treatment × sex interaction $P < 0.05$).

In addition to number, microglial activity can also be ascertained from cell shape.[18,33] Thus, we next used the MicrogliaMorphology pipeline to objectively characterize microglial phenotypic state in vehicle-treated hemoglobin control and SCD mice as well as minocycline-treated SCD mice.[42] Four reproducible morphological clusters were derived from principal component analysis of microglial fractal skeletons (**Figs. 4A and B**; Supplemental Fig. 1, http://links.lww.com/PAIN/C503): ameboid, hypertrophic, ramified, and rod-like. Although minocycline treatment did not alter the proportion of microglial phenotypic in male mice (**Fig. 4B**), microglial treatment resulted in significant sex-specific alterations. Cluster proportions were used to run a partial least squares discrimination analysis (PLS-DA) between the sexes within each treatment group. Minimal separation was observed between vehicle-treated animals, but a clear sex-dependent separation was observed in minocycline-treated mice, suggesting that drug treatment unmasks or amplifies sex-specific differences in microglial state composition (**Fig. 4C**). To determine which cluster – if any – was most responsible for the sex-dependent minocycline effects, Cliff delta effect size was calculated and compared between the sexes (**Fig. 4D**). This analysis consistently identified rod-like (**Fig. 4E**) and ramified (**Fig. 4F**) microglia as having the largest effect on the microglial reorganization that occurs after minocycline treatment. In summary, we conclude that SCD factors induce spinal microgliosis in a sex-dependent manner. These effects are further compounded by the sexually dimorphic effects of minocycline treatment on SCD spinal microglia.

3.4. Minocycline analgesia results, in part, from effects on male sickle cell disease mouse gut microbiome

Given that minocycline had effects on both spleen size and colon length in SCD mice, we reasoned that minocycline-induced changes in the gut microbiome may also contribute to the sex-specific analgesia observed in male SCD mice. To directly test this hypothesis, a series of FMT experiments was performed. In this paradigm, the gut microbiome of sex-matched C57BL/6 mice was altered by oral administration of resuspended fecal material collected from either vehicle- or minocycline-treated SCD mice (**Fig. 5A**). Hind paw mechanical sensitivity was measured in FMT recipients at various points throughout the

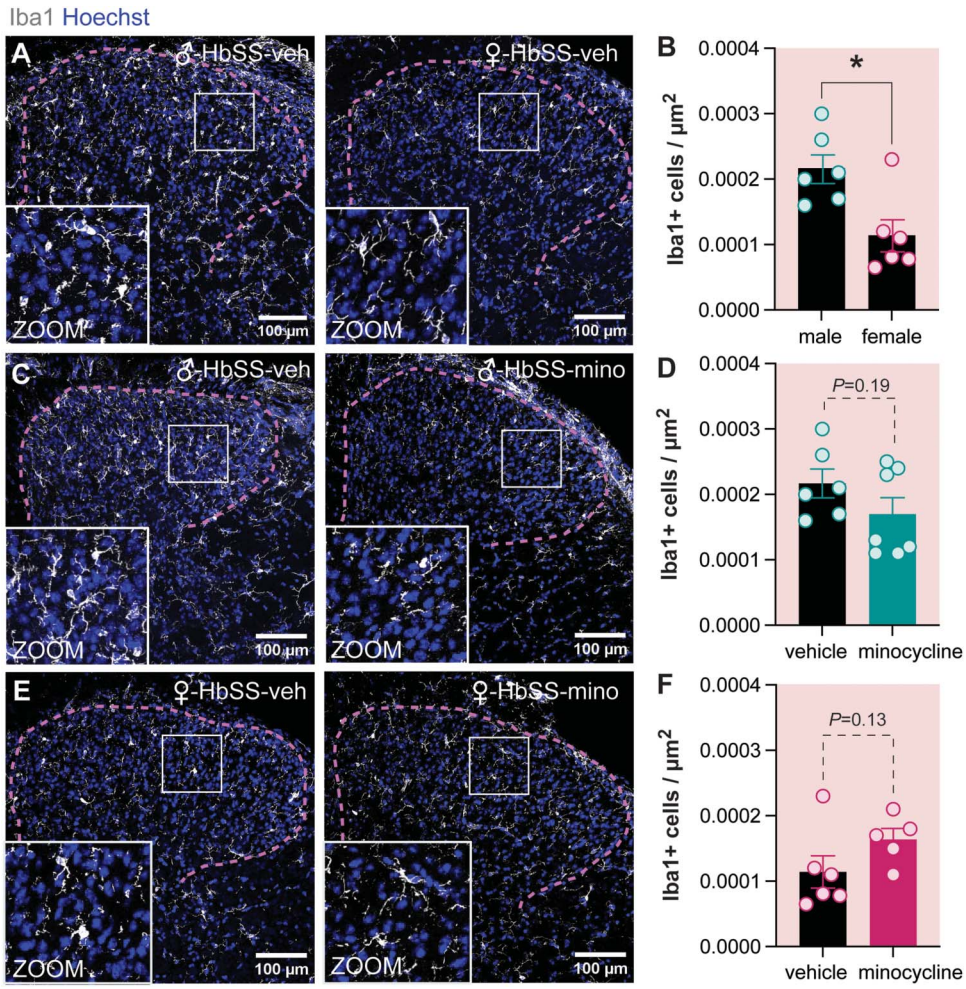

Figure 3. Sex-specific effects of SCD and minocycline treatment on spinal microgliosis. Representative images (A, C, E) and quantification (B, D, F) of Iba1+ microglia in the dorsal horn of (A, B) vehicle-treated male and female HbSS (SCD) mice, (C, D) vehicle- and minocycline-treated male HbSS mice, and (E, F) vehicle- and minocycline-treated female HbSS mice. *$P < 0.05$, unpaired t test with Welch correction. HbAA, homozygous for wildtype β-globin; HbSS, homozygous for sickle β-globin; SCD, sickle cell disease.

paradigm to determine if changes in the gut microbiota alter pain-like behaviors. In line with previous work,[4,41] male C57BL/6 mice that received vehicle-treated SCD FMT developed hind paw mechanical hypersensitivity that persisted for >1 week after the last FMT. In contrast, male mice that received FMT from minocycline-treated SCD donors did not develop the same mechanical allodynia phenotype (**Figs. 5B and C**). Different observations were made in female mice. Fecal microbiota transplant from both vehicle- and minocycline-treated SCD female mice induced pain in female FMT recipients (**Figs. 5B and C**). Notably, mechanical hypersensitivity persisted in female FMT recipients for >2 weeks, regardless of FMT donor treatment. Thus, in addition to having differential effects on spinal microgliosis, minocycline analgesia in male SCD mice can also be attributed to changes in the gut microbiome that do not occur in female SCD mice.

3.5. Minocycline does not exert sex-specific antibiotic effects on bacterial phyla

Given the robust difference in male and female behavior after FMT, we examined whether minocycline treatment induces sex-specific antibiotic effects in SCD mice. Before measuring the relative abundance of individual bacteria, cecum size and fecal DNA content were compared between mice used as FMT donors. Increased cecum size was noted in both minocycline-treated HbAA (hemoglobin control) male (**Fig. 6A**) and female (**Fig. 6B**) mice. This was expected as increased cecum size is a well-documented indicator of antibiotic efficacy. Increased cecum size was not observed in minocycline-treated SCD mice, most likely because vehicle-treated SCD mice trended to have heavier ceca than hemoglobin control mice. In addition to increasing cecum size, minocycline treatment also increased DNA concentrations detected in male hemoglobin control mouse feces, again providing additional support for the antibiotic effects of minocycline (**Fig. 6C**). This same observation was not made in feces collected from female SCD or hemoglobin control mice (**Fig. 6D**).

To specifically examine if minocycline alters SCD intestinal bacterial populations in a sex-specific manner, quantitative real-time PCR was used to quantify the relative abundance of the primary bacterial phyla present in mouse intestines. As predicted, *Bacteroidetes* and *Firmicutes* were the most abundant phyla detected in both vehicle- and minocycline-treated SCD feces; members of phyla *Actinobacteria* and *Verrucomicrobia* were present at much lower levels (**Fig. 6E**). A subsequent analysis on individual phyla was completed to better assess if sex-specific effects of minocycline could be detected. Indeed,

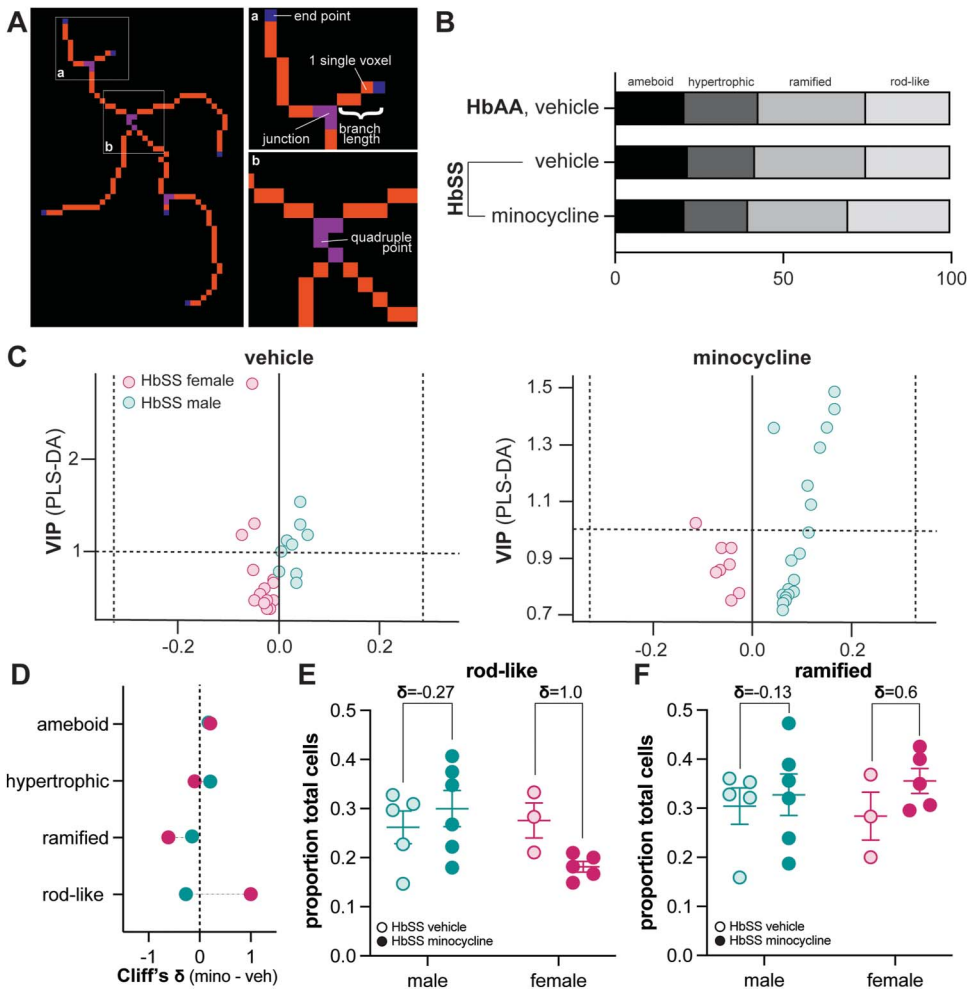

Figure 4. Sex-specific effects of minocycline treatment on spinal microglia morphology. (A) Representative image of microglial morphological features quantified using MicrogliaMorphology pipeline. (B) Proportion of total microglia belonging to each phenotype cluster for all male experimental groups. (C) Partial least squares discriminant analysis (PLS-DA) using the 4 cluster proportions as predictors and sex as the response variable. Analysis was performed separately within each treatment condition. (D) Cliff delta value comparison between sexes and within each cluster. The vertical dashed line indicates no treatment effect (δ = 0). Cliff delta for (E) rod-like and (F) ramified microglia reported on a sex basis.

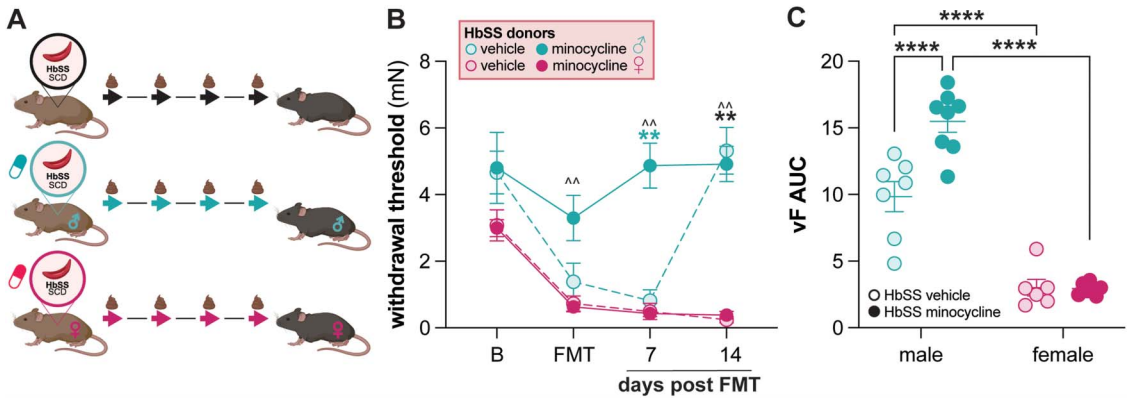

Figure 5. Minocycline-induced changes in the male SCD gut microbiome contribute to sex-specific analgesia. (A) Schematic of fecal microbiota transplant (FMT) experiments. Fecal material was collected from vehicle- or minocycline-treated SCD (HbSS) mice and then orally administered to naïve sex-matched C57BL/6 recipients every other day over the course of 7 days. (B) Hind paw mechanical withdrawal thresholds of FMT recipients throughout the paradigm (B): baseline; N = 6-8; Bonferroni post-hoc tests: minocycline male vs female ^^$P < 0.01$, male minocycline vs vehicle **$P < 0.01$, vehicle male vs female **$P < 0.01$. (C) Area under the curve (AUC) calculation for von Frey behavioral assessments during entirety of FMT paradigm. HbAA, homozygous for wildtype β-globin; HbSS, homozygous for sickle β-globin; SCD, sickle cell disease.

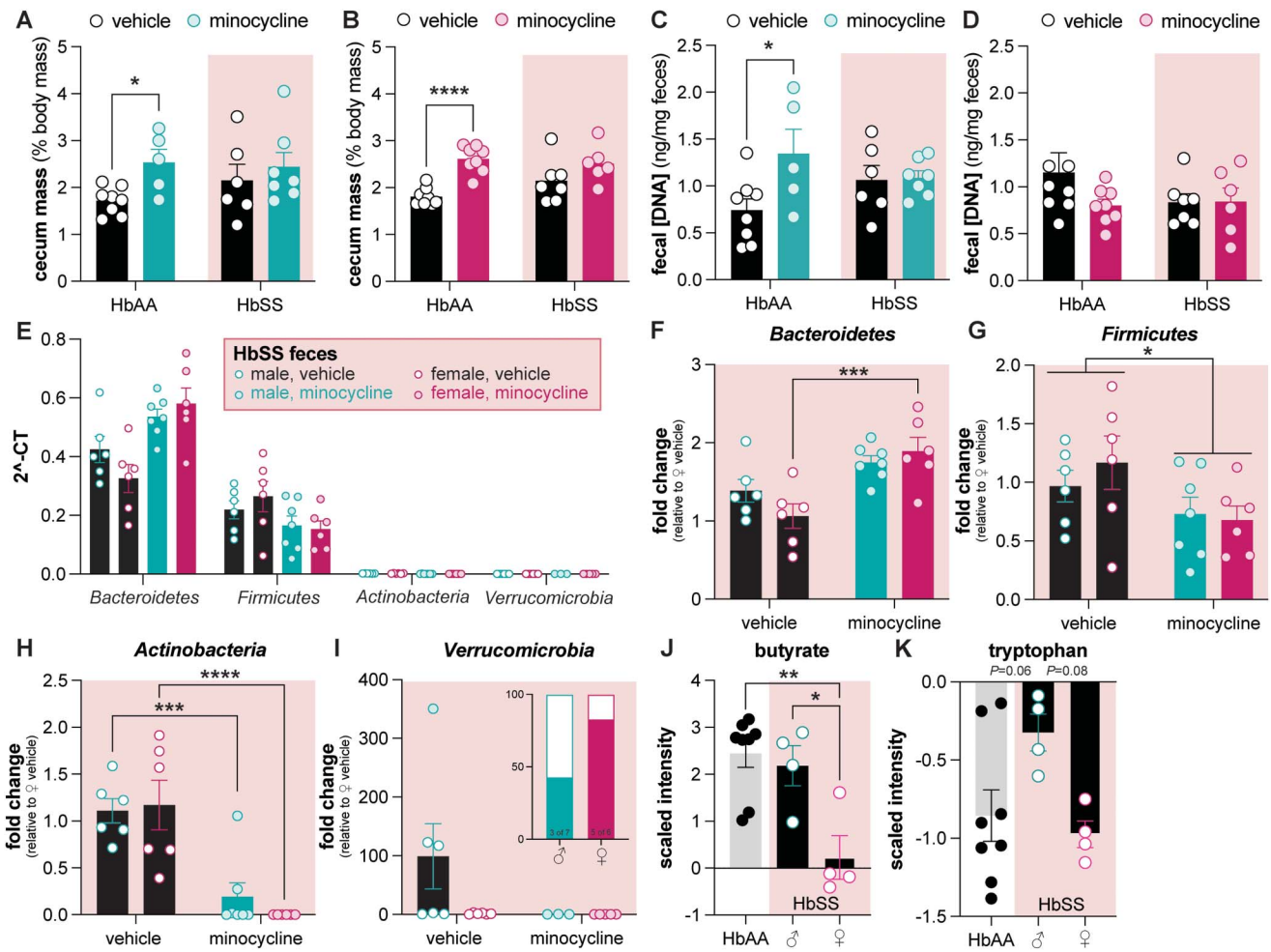

Figure 6. Minocycline-induced changes in the SCD gut microbiota. Male (teal) and female (magenta) SCD (HbSS) and hemoglobin control (HbAA) mice were maintained on ad libitum minocycline treatment (100 mg/kg) for 6 days. After treatment, relative cecum mass for (A) male and (B) female mice and DNA content in feces from (C) male and (D) female mice was recorded. (E) Relative abundance of bacterial phyla in feces collected from vehicle- and minocycline-treated SCD mice. Relative abundance of (F) *Bacteroidetes*, (G) *Firmicutes* (2-way ANOVA overall effect of treatment $^{*}P < 0.05$), (H) *Actinobacteria*, and (I) *Verrucomicrobia* in feces collected from vehicle- and minocycline-treated SCD mice. Panel (J) inset illustrates % of minocycline-treated male (teal) and female (magenta) mice with detectable *Verrucomicrobia* in feces. Relative concentration of (J) butyrate and (K) tryptophan in feces collected from vehicle-treated HbAA hemoglobin control mice, as well as male and female vehicle-treated HbSS SCD mice. Unless otherwise noted, Bonferroni post-hoc tests: $^{*}P < 0.05$, $^{***}P < 0.001$, $^{****}P < 0.0001$. HbAA, homozygous for wildtype β-globin; HbSS, homozygous for sickle β-globin; SCD, sickle cell disease.

minocycline treatment significantly increased the abundance of *Bacteroidetes* in female SCD feces but did not have the same effect in male SCD mice (**Fig. 6F**). This was the only sex difference observed in our analysis. Minocycline treatment decreased the relative abundance of *Firmicutes* and *Actinobacteria* in both male and female SCD mice (**Figs. 6G and H**). Finally, given the highly variable levels of *Verrucomicrobia* detected across samples, there were no statistical differences noted between treatment groups (**Fig. 6I**). Given the relatively similar effects of minocycline on male and female bacterial populations, we next examined sex differences in fecal metabolites. In a reanalysis of our previously published data set, we found that 202 of 1030 metabolites detected in SCD mouse feces differed between males and females (Supp. Table 1, http://links.lww.com/PAIN/C504). Of particular note were the short chain fatty acid butyrate and essential amino acid tryptophan. Female SCD mice had significantly less butyrate in their feces as compared to both male SCD mice and HbAA hemoglobin controls (**Fig. 6J**). In contrast, male SCD mice had higher levels of tryptophan in their feces when compared with HbAA controls and female SCD mice (**Fig. 6K**). Future studies should investigate if minocycline treatment affects the abundance of these critical gut metabolites in a sex-specific fashion.

4. Discussion

New analgesics are desperately needed for those diagnosed with SCD. To this end, we determined that minocycline may provide chronic pain relief for males suffering from SCD, but not females. This is not the first time male-specific minocycline analgesia has been reported in preclinical pain models. Minocycline effectively alleviates pain in male—but not female—rodents that have received intraplantar injection of formalin[14] or complete Freund adjuvant,[69] intra-articular injection of high mobility group box-1 protein (HMGB1),[62] collagen antibody–induced arthritis,[24] tibia fracture,[31] early-life injury-induced priming,[57] stress-exacerbated incisional pain,[75] chronic constriction injury (CCI),[14,52] and spared nerve injury (SNI).[69]

Although there are many mechanisms through which minocycline can alleviate pain,[27] this sex specificity has largely been attributed to the drug's inhibitory effects on microglia in the male spinal cord. Unlike many previous studies that reported similar levels of microgliosis between sexes after peripheral injury, here

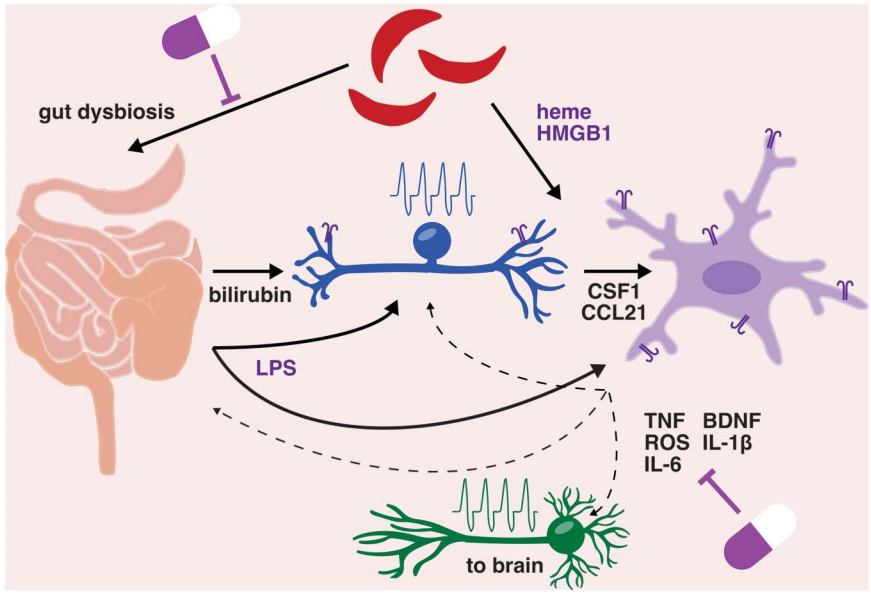

Figure 7. Potential mechanisms of minocycline analgesia in SCD. Summary of how minocycline treatment may influence complex interactions between sickled red blood cells, intestines, primary sensory neurons (blue), spinal microglia (purple), and dorsal horn neurons (green) in SCD. Note that all molecules and features (ie, gut dysbiosis and neuronal activity) listed in image have been reported as elevated in patients with SCD or mouse models. SCD, sickle cell disease.

we observed sex-specific increases in spinal microgliosis; male SCD mice have more spinal microglia than females. In addition, we found that minocycline treatment significantly shifted the microglial phenotypic differences observed between the sexes, most notably altering the abundance of rod-like and ramified microglia. This is the first time sex-specific microglial changes have been reported in transgenic SCD mice. Previous studies have reported increased spinal[71] and hippocampal[34] microgliosis in SCD mice when compared with hemoglobin controls. Of note, minocycline is currently in phase 1 clinical trials for sickle cell neurocognitive impairments attributed to this hippocampal—and additional supraspinal site—microgliosis (NCT05605366). In detailed reading of the methods sections, however, the existing preclinical studies only examined tissues and behavioral outcomes from 1 sex; spinal microgliosis was only assessed in female SCD/control tissue,[71] and hippocampal microgliosis and associated cognitive deficits were only assessed in male SCD/control tissue.[34] Although not only expressed in microglia, spinal toll-like receptor 4 (TLR4) has been found to drive pain specifically in male but not female mice.[68] Expression of TLR4 has been shown to be increased in SCD mouse spinal cords,[48] but in the singular study that reported this finding, sex-specific analysis of spinal TLR4 expression was not presented.[48] This same study also found that systemic pharmacological inhibition and genetic knockdown of TLR4 alleviated pain in male and female SCD mice, but again, these behavioral results were not segregated by sex. Thus, in summary, male-specific increases in spinal microgliosis may be a previously unreported feature in chronic SCD that provides unique opportunities for future therapeutic development.

Although not specifically addressed in our current study, there are several explanations for what could be driving male-specific increases in spinal microgliosis (summary of hypotheses featured in **Fig. 7**). First is spinal colony-stimulating factor 1 (CSF1) signaling. Colony-stimulating factor 1 (also known as macrophage colony-stimulating factor; M-CSF) is a cytokine secreted by many cell types, including injured peripheral sensory neurons.[30] When intrathecally injected into naïve mice, CSF1 induces pain and microglial activation, but only in male animals.[45] In female mice, intrathecal CSF1 induces expansion of regulatory T-cell (Tregs) populations, cells that subsequently prevent microglial activation.[45] Notably, both CSF1[50] and Tregs[73] are increased in blood collected from individuals with SCD. Colony-stimulating factor 1 is also elevated in transgenic SCD mice[50]; to our knowledge, no study has examined Treg populations in SCD animals. Thus, it is possible that in SCD, elevated spinal CSF1—which may come from either "injured" peripheral nociceptors[64] or additional cell types—selectively induces microglial activation in males.

A second possible mechanism for male-specific microgliosis in SCD is spinal activity of extracellular HMGB1. High mobility group box-1 protein is classic damage-associated molecular pattern (DAMP). Normally found in the nucleus, HMGB1 is secreted from necrotic cells[67] and released by activated immune cells and peripheral nociceptors.[39,78,79] Notably, individuals and mice with SCD have elevated levels of HMGB1 in circulation that is further increased during acute pain episodes.[77] Previously, intrathecal injection of HMGB1 was found to induce similar pain-like behaviors in male and female mice,[1] but in vitro exposure to HMGB1 induced sex-specific increases in microglial expression of *Tnf*, *Ccl2*, *Il1b*, and *Il6*.[2] Receptors for these factors are expressed by neuronal and immune cells in the dorsal horn—including the microglia from whence they came. Thus, it is possible that in SCD, elevated levels of HMGB1 perpetuate a sex-specific, feed-forward exacerbation of microgliosis that may only be remedied by neutralizing circulating HMGB1.

Although we did not observe a statistically significant change in male microglial number or morphology after acute minocycline treatment, it is possible that drug treatment altered the expression and release of compounds from microglia in a sex-dependent manner. Indeed, despite observing similar levels of microgliosis between sexes after peripheral injury, several groups have identified key, sex-specific transcriptional and proteomic changes in the spinal cord after minocycline treatment. For

example, in the landmark paper that first described sex-specific immune cell pain modulation, microglial brain-derived neurotrophic factor (BDNF) was critical for pain in male mice but not females.[69] Like every other proinflammatory or pronociceptive compound mentioned in this manuscript, BDNF is also elevated in SCD plasma.[38] It is unknown if similar increases in microglial-BDNF exist in SCD, but given that the ultimate effect of elevated spinal BDNF signaling is activation of TrkB receptors and subsequent hyperexcitability of dorsal horn neurons—a phenomenon that has been reported in SCD mice[12]—future studies should explore the potential sex-specific analgesic efficacy of TrkB inhibitors in SCD.

In addition to decreased BDNF release in the male spinal cord, minocycline treatment has also been shown to result in male-specific *increases* in spinal haptoglobin and hemopexin.[2] This is incredibly relevant to the current studies given that haptoglobin and hemopexin are, respectively, free hemoglobin and heme scavengers. Individuals and mouse models with SCD have chronically elevated levels of free heme and decreased levels of hemopexin because of the excessive hemolysis that is characteristic of SCD.[48,58,72,74] Elevated heme drives chronic SCD pain by activating TLR4; double transgenic SCD/TLR4 knockout mice are prevented against the development of severe chronic mechanical, thermal, and deep tissue pain and heme-induced exacerbations of this pain.[48] Thus, the male-specific minocycline analgesia observed in the current studies may result from decreased free-heme and subsequent dampening of TLR4-dependent nociceptive signaling in the spinal cord.

Here, we demonstrate, for the first time, that sex-specific minocycline analgesia also results from changes in the intestinal milieu. Fecal microbiota transplant from minocycline-treated male SCD mice did not induce pain in recipients; FMT from vehicle-treated male or female SCD mice as well as minocycline-treated female SCD mice induced mechanical hypersensitivity in recipients, similar to previous reports.[4,41] There are many prokaryotic and eukaryotic factors in the SCD gut that could be impacted by minocycline treatment. First is the gut microbiota, or the bacteria that reside within the intestines. Although we did not observe robust, sex-specific antibiotic effects of minocycline in the current experiments, future studies should more thoroughly test this hypothesis using species-level gene sequencing. Sex-specific effects of antibiotics have been previously reported in rodents; administration of vancomycin, ciprofloxacin-metronidazole, and a four-drug antibiotic cocktail all lead to sex-specific changes in gut bacteria[26,59] or metabolites.[26] Sex-specific changes in the gut microbiota may also lead to differential effects on the immune system, in particular macrophages which are another known target of minocycline activity.[27]

Host and bacterial metabolites are the second factor that may be modulated by minocycline in a sex-dependent fashion. In our previous examination of the SCD mouse gut microbiome, we did not observe sex differences in alpha- or beta-diversity. A secondary analysis of our metabolomic data,[4] however, revealed significant differences between relative compound levels in male and female SCD mouse feces. Butyrate and tryptophan are just 2 of the noteworthy molecules found to be present in different levels in male and female SCD guts. Butyrate is a bacterial-derived short-chain fatty acid that is critical for gut barrier integrity.[60] The critically low levels of butyrate observed in female SCD mice may provide a partial explanation for the shorter colon length observed in these same animals. Given that minocycline reversed colonic shortening—a classic indicator of colonic inflammation—it is possible that levels of butyrate are also increased in feces collected specifically from minocycline-treated female SCD mice. In contrast, male SCD mice had higher levels of tryptophan in their feces when compared with both female SCD mice and hemoglobin controls. Given that tryptophan metabolites have been shown to have antinociceptive and anti-inflammatory properties,[51,53,80] this may indicate that insufficient tryptophan metabolism is occurring specifically in the male SCD gut. Minocycline treatment may prevent the growth of tryptophan-metabolizing competitors, thus allowing for increased tryptophan breakdown, and ultimately decreased gut inflammation.

In closing, these studies demonstrate the analgesic efficacy of minocycline in male SCD mice, and, for the first time, imply that the antibiotic effects of minocycline may also lead to sex-specific analgesia. This is perhaps not surprising given the complex multidirectional interactions between the immune system, gut microbiome, and peripheral nervous system (**Fig. 7**). In addition, these results provide critical sex-specific insight into SCD pain biology. The observation that spinal microgliosis specifically occurs in male mice should encourage a reexamination of accepted SCD pain mechanisms on the basis of sex. Uncovering sexually dimorphic pain processes in this disease state will ultimately allow for more effective, personalized analgesics.

Conflict of interest statement

The authors have no conflict of interest to declare.

Acknowledgements

The authors would like to thank Nya Gayluak and Victor Cho for assisting with tissue collection, Joe Lombardo and the UT Dallas Imaging and Histology Core for assistance with confocal image collection and analysis, Dr. Michael Burton and laboratory for Iba1 staining protocol, and Dr. Lena Nguyen for real-time qPCR system and NanoDrop access. Select illustrations were created with BioRender.com. Raw metabolomic data are available upon request (email corresponding author Sadler). This work was supported by funding from the National Institutes of Health (grant R00 HL155791 to K.E.S.) and the Rita Allen Foundation (Award in Pain to K.E.S.).

Supplemental digital content

Supplemental digital content associated with this article can be found online at http://links.lww.com/PAIN/C503 and http://links.lww.com/PAIN/C504.

Supplemental video content

A video abstract associated with this article can be found on the PAIN Web site.

Article history:
Received 5 September 2025
Received in revised form 19 February 2026
Accepted 23 February 2026
Available online 26 May 2026

References

[1] Agalave NM, Larsson M, Abdelmoaty S, Su J, Baharpoor A, Lundbäck P, Palmblad K, Andersson U, Harris H, Svensson CI. Spinal HMGB1 induces TLR4-mediated long-lasting hypersensitivity and glial activation and regulates pain-like behavior in experimental arthritis. PAIN 2014;155:1802–13.

[2] Agalave NM, Rudjito R, Farinotti AB, Khoonsari PE, Sandor K, Nomura Y, Szabo-Pardi TA, Urbina CM, Palada V, Price TJ, Erlandsson Harris H, Burton MD, Kultima K, Svensson CI. Sex-dependent role of microglia in disulfide high mobility group box 1 protein-mediated mechanical hypersensitivity. PAIN 2021;162:446–58.
[3] Alvarez-Argote J, Dlugi TA, Sundararajan T, Kleynerman A, Faber ML, McKillop WM, Medin JA. Pathophysiological characterization of the Townes mouse model for sickle cell disease. Translational Res 2023;254:77–91.
[4] Brandow AM, Atkinson SN, Manjarres Z, Ehlers VL, Pratt ML, Mehta I, Mudunuri S, Kappagantu A, Shiers SI, Mazhar K, Simms MA, Alhendi S, Sheshadri A, Cervantes AM, Reese JC, Tavares-Ferreira D, Sankaranarayanan I, Schaub MK, Waltz TB, Hayward M, Rodríguez García DM, Dussor G, Salzman NH, Palmer KL, Stucky CL, Price TJ, Sadler KE. Gut microbiota and metabolites drive chronic sickle cell disease pain in mice. Cell Host Microbe 2025;33:1703–14.e8.
[5] Brandow AM, Carroll CP, Creary S, Edwards-Elliott R, Glassberg J, Hurley RW, Kutlar A, Seisa M, Stinson J, Strouse JJ, Yusuf F, Zempsky W, Lang E. American Society of Hematology 2020 guidelines for sickle cell disease: management of acute and chronic pain. Blood Adv 2020;4:2656–701.
[6] Brandow AM, Zappia KJ, Stucky CL. Sickle cell disease: a natural model of acute and chronic pain. PAIN 2017;158:S79–84.
[7] Brenner DS, Golden JP, Gereau RW. A novel behavioral assay for measuring cold sensation in mice. PLoS One 2012;7:e39765.
[8] Brim H, Taylor J, Abbas M, Vilmenay K, Daremipouran M, Varma S, Lee E, Pace B, Song-Naba WL, Gupta K, Nekhai S, O'Neil P, Ashktorab H. The gut microbiome in sickle cell disease: characterization and potential implications. PLoS One 2021;16:e0255956.
[9] Brim H, Vilmenay K, Atefi N, Abdul A, Daremipouran M, Lee EL, Gillevet PM, O'Neal P, Ashktorab H. GUT microbiome analysis reveals major dysbiosis in sickle cell diseases patients with a prevalence of veillonella strains. Gastroenterology 2017;152:S631.
[10] Cain DM, Vang D, Simone DA, Hebbel RP, Gupta K. Mouse models for studying pain in sickle cell disease: effects of strain, age, and acuteness. Br J Haematol 2012;156:535–44.
[11] Carroll CP, Brandow AM. Chronic pain: prevalence and management. Hematol Oncol Clin North Am 2022;36:1151–65.
[12] Cataldo G, Rajput S, Gupta K, Simone DA. Sensitization of nociceptive spinal neurons contributes to pain in a transgenic model of sickle cell disease. PAIN 2015;156:722–30.
[13] Chaplan SR, Bach FW, Pogrel JW, Chung JM, Yaksh TL. Quantitative assessment of tactile allodynia in the rat paw. J Neurosci Methods 1994; 53:55–63.
[14] Chen G, Luo X, Qadri MY, Berta T, Ji RR. Sex-dependent glial signaling in pathological pain: distinct roles of spinal microglia and astrocytes. Neurosci Bull 2018;34:98–108.
[15] Conran N, Belcher JD. Inflammation in sickle cell disease. Clin Hemorheol Microcirc 2018;68:263–99.
[16] Cowie AM, Moehring F, O'Hara C, Stucky CL. Optogenetic inhibition of CGRPα sensory neurons reveals their distinct roles in neuropathic and incisional pain. J Neurosci 2018;38:5807–25.
[17] Dampier C, Palermo TM, Darbari DS, Hassell K, Smith W, Zempsky W. AAPT diagnostic criteria for chronic sickle cell disease pain. J Pain 2017; 18:490–8.
[18] Davis LK, Anders MM, Guerin SP, Khoury SE, Thompson LM, Darling JS, Gore AC, Fonken LK. Sex differences in microglia morphology and function across the lifespan are mediated by the early hormone environment. Brain Behav Immun 2026;132:106187.
[19] Delgadinho M, Ginete C, Santos B, Mendes J, Miranda A, Vasconcelos J, Brito M. Microbial gut evaluation in an angolan paediatric population with sickle cell disease. J Cell Mol Med 2022;26:5360–8.
[20] DeVeaux SA, Vyshnya S, Propsom K, Gbotosho OT, Singh AS, Horning RZ, Sharma M, Jegga AG, Niu L, Botchwey EA, Hyacinth HI. Neuroinflammation underlies the development of social stress induced cognitive deficit in male sickle cell mice. Exp Biol Med 2024;249:10361.
[21] Dike CR, Hanson C, Davies HD, Obaro S, Yu F, Harper J, Grace H, Lebensburger J, Raulji C, Ma J, Mannon P. The relationship between nutrition, gut dysbiosis, and pediatric sickle cell pain outcomes: a pilot study. Pediatr Blood Cancer 2023;70:e30397.
[22] Dixon WJ. The up-and-down method for small samples. J Am Stat Assoc 1965;60:967–78.
[23] Fan CY, McAllister BB, Stokes-Heck S, Harding EK, Pereira de Vasconcelos A, Mah LK, Lima LV, van den Hoogen NJ, Rosen SF, Ham B, Zhang Z, Liu H, Zemp FJ, Burkhard R, Geuking MB, Mahoney DJ, Zamponi GW, Mogil JS, Ousman SS, Trang T. Divergent sex-specific pannexin-1 mechanisms in microglia and T cells underlie neuropathic pain. Neuron 2025;113:896–911.e9.
[24] Fernandez-Zafra T, Gao T, Jurczak A, Sandor K, Hore Z, Agalave NM, Su J, Estelius J, Lampa J, Hokfelt T, Wiesenfeld-Hallin Z, Xu X, Denk F, Svensson CI. Exploring the transcriptome of resident spinal microglia after collagen antibody-induced arthritis. PAIN 2019;160:224–36.
[25] Field JJ, Ballas SK, Campbell CM, Crosby LE, Dampier C, Darbari DS, McClish DK, Smith WR, Zempsky WT. AAAPT diagnostic criteria for acute sickle cell disease pain. J Pain 2019;20:746–59.
[26] Gao H, Shu Q, Chen J, Fan K, Xu P, Zhou Q, Li C, Zheng H. Antibiotic exposure has sex-dependent effects on the gut microbiota and metabolism of short-chain fatty acids and amino acids in mice. mSystems 2019;4:e00048-19.
[27] Garrido-Mesa N, Zarzuelo A, Gálvez J. What is behind the non-antibiotic properties of minocycline? Pharmacol Res 2013;67:18–30.
[28] Gaudio E, Taddei G, Vetuschi A, Sferra R, Frieri G, Ricciardi G, Caprilli R. Dextran sulfate sodium (DSS) colitis in rats: clinical, structural, and ultrastructural aspects. Dig Dis Sci 1999;44:1458–75.
[29] Glaros A, Brandow AM. Neuropathic pain in sickle cell disease: measurement and management. Hematol Am Soc Hematol Education Program 2020;2020:553–61.
[30] Guan Z, Kuhn JA, Wang X, Colquitt B, Solorzano C, Vaman S, Guan AK, Evans-Reinsch Z, Braz J, Devor M, Abboud-Werner SL, Lanier LL, Lomvardas S, Basbaum AI. Injured sensory neuron–derived CSF1 induces microglial proliferation and DAP12-dependent pain. Nat Neurosci 2016 19:94–101.
[31] Guo T, Shi X, Li W, Wei T, Clark J, Kingery WS. Sex differences in the temporal development of pronociceptive immune responses in the tibia fracture mouse model. PAIN 2019;160:2013–27.
[32] Guo X, Xia X, Tang R, Zhou J, Zhao H, Wang K. Development of a real-time PCR method for Firmicutes and Bacteroidetes in faeces and its application to quantify intestinal population of obese and lean pigs. Lett Appl Microbiol 2008;47:367–73.
[33] Han J, Fan Y, Zhou K, Blomgren K, Harris RA. Uncovering sex differences of rodent microglia. J Neuroinflammation 2021;18:74.
[34] Hardy RA, Rached NA, Jones JA, Archer DR, Hyacinth HI. Role of age and neuroinflammation in the mechanism of cognitive deficits in sickle cell disease. Exp Biol Med 2020;246:106–20.
[35] Hillery CA, Kerstein PC, Vilceanu D, Barabas ME, Retherford D, Brandow AM, Wandersee NJ, Stucky CL. Transient receptor potential vanilloid 1 mediates pain in mice with severe sickle cell disease. Blood 2011;118:3376–83.
[36] Hogan Q, Sapunar D, Modric-Jednacak K, McCallum JB. Detection of neuropathic pain in a rat model of peripheral nerve injury. Anesthesiology 2004;101:476–87.
[37] Huse SM, Dethlefsen L, Huber JA, Welch DM, Relman DA, Sogin ML. Exploring microbial diversity and taxonomy using SSU rRNA hypervariable tag sequencing. PLoS Genet 2008;4:e1000255.
[38] Hyacinth HI, Gee BE, Adamkiewicz TV, Adams RJ, Kutlar A, Stiles JK, Hibbert JM. Plasma BDNF and PDGF-AA levels are associated with high TCD velocity and stroke in children with sickle cell anemia. Cytokine 2012; 60:302–8.
[39] Ito I, Fukazawa J, Yoshida M. Post-translational methylation of high mobility group box 1 (HMGB1) causes its cytoplasmic localization in neutrophils. J Biol Chem 2007;282:16336–44.
[40] Karahan F, Yilmaz SS, Bayrakdar F, Tezol Ö, Kuyucu N, Kiliç S, Türkegün M, Ünal S. Evaluation of intestinal microbiota in children with sickle cell disease. J Pediatr Hematol Oncol 2023;45:E904–9.
[41] Kashyap Y, Wang ZJ. Gut microbiota dysbiosis alters chronic pain behaviors in a humanized transgenic mouse model of sickle cell disease. PAIN 2024;165:423–39.
[42] Kim J, Pavlidis P, Ciernia AV. Development of a high-throughput pipeline to characterize microglia morphological states at a single-cell resolution. eNeuro 2024;11:ENEURO.0014-24.2024.
[43] Kohli DR, Li Y, Khasabov SG, Gupta P, Kehl LJ, Ericson ME, Nguyen J, Gupta V, Hebbel RP, Simone DA, Gupta K. Pain-related behaviors and neurochemical alterations in mice expressing sickle hemoglobin: modulation by cannabinoids. Blood 2010;116:456–65.
[44] Kommineni S, Bretl DJ, Lam V, Chakraborty R, Hayward M, Simpson P, Cao Y, Bousounis P, Kristich CJ, Salzman NH. Bacteriocin production augments niche competition by enterococci in the mammalian gastrointestinal tract. Nature 2015;526:719–22.
[45] Kuhn JA, Vainchtein ID, Braz J, Hamel K, Bernstein M, Craik V, Dahlgren MW, Ortiz-Carpena J, Molofsky AB, Molofsky AV, Basbaum AI. Regulatory t-cells inhibit microglia-induced pain hypersensitivity in female mice. Elife 2021;10:e69056.
[46] Ledeboer A, Sloane EM, Milligan ED, Frank MG, Mahony JH, Maier SF, Watkins LR. Minocycline attenuates mechanical allodynia and proinflammatory cytokine expression in rat models of pain facilitation. PAIN 2005;115:71–83.
[47] Lei J, Benson B, Tran H, Ofori-Acquah SF, Gupta K. Comparative analysis of pain behaviours in humanized mouse models of sickle cell anemia. PLoS One 2016;11:e0160608.

[48] Lei J, Paul J, Wang Y, Gupta M, Vang D, Thompson S, Jha R, Nguyen J, Valverde Y, Lamarre Y, Jones MK, Gupta K. Heme causes pain in sickle mice via toll-like receptor 4-mediated reactive oxygen species- and endoplasmic reticulum stress-induced glial activation. Antioxid Redox Signaling 2021;34:279–93.
[49] Lim SH, Morris A, Li K, Fitch AC, Fast L, Goldberg L, Quesenberry M, Sprinz P, Methé B. Intestinal microbiome analysis revealed dysbiosis in sickle cell disease. Am J Hematol 2018;93:E91–3.
[50] Liu Y, Su S, Shayo S, Bao W, Pal M, Dou K, Shi PA, Aygun B, Campbell-Lee S, Lobo CA, Mendelson A, An X, Manwani D, Zhong H, Yazdanbakhsh K. Hemolysis dictates monocyte differentiation via two distinct pathways in sickle cell disease vaso-occlusion. J Clin Invest 2023; 133:e172087.
[51] Maëva M, Elodie B, Nathalie R, Manon D, Marjolène S, Valentine D, Morgane M, Ivan W, Frédéric D, Romain V, Mathieu M, Esther BN, Catherine G, Nicolas B, Denis A, Philippe P, Harry S, Jean-Marc C, Philippe L, Valérie L, Mathilde B, Frédéric Antonio C. AhR/IL-22 pathway as new target for the treatment of post-infectious irritable bowel syndrome symptoms. Gut Microbes 2022;14:2022997.
[52] Mapplebeck JCS, Dalgarno R, Tu YS, Moriarty O, Beggs S, Kwok CHT, Halievski K, Assi S, Mogil JS, Trang T, Salter MW. Microglial P2X4R-evoked pain hypersensitivity is sexually dimorphic in rats. PAIN 2018;159:1752–63.
[53] Marafini I, Monteleone I, Laudisi F, Monteleone G. Aryl hydrocarbon receptor signalling in the control of gut inflammation. Int J Mol Sci 2024; 25:4527.
[54] Martell MJ, Boothe JH. The 6-Deoxytetracyclines. VII. Alkylated aminotetracyclines possessing unique antibacterial activity. J Med Chem 1967;10:44–6.
[55] Milligan E, Zapata V, Schoeniger D, Chacur M, Green P, Poole S, Martin D, Maier SF, Watkins LR. An initial investigation of spinal mechanisms underlying pain enhancement induced by fractalkine, a neuronally released chemokine. Eur J Neurosci 2005;22:2775–82.
[56] Mittal AM, Lamarre YY, Gupta K. Observer based objective pain quantification in sickle mice using grimace scoring and body parameters. Blood 2014;124:4907.
[57] Moriarty O, Tu YS, Sengar AS, Salter MW, Beggs S, Walker SM. Priming of adult incision response by early-life injury: neonatal microglial inhibition has persistent but sexually dimorphic effects in adult rats. J Neurosci 2019;39:3081–93.
[58] Muller-Eberhard U, Javid J, Liem HH, Hanstein A, Hanna M. Brief report: plasma concentrations of hemopexin, haptoglobin and heme in patients with various hemolytic diseases. Blood 1968;32:811–5.
[59] Parodi G, Leite G, Pimentel ML, Barlow GM, Fiorentino A, Morales W, Pimentel M, Weitsman S, Mathur R. The response of the rodent gut microbiome to broad-spectrum antibiotics is different in males and females. Front Microbiol 2022;13:897283.
[60] Peng L, Li ZR, Green RS, Holzmanr IR, Lin J. Butyrate enhances the intestinal barrier by facilitating tight junction assembly via activation of AMP-activated protein kinase in Caco-2 cell monolayers. J Nutr 2009; 139:1619–25.
[61] Redin GS. Antibacterial activity in mice of minocycline, a new tetracycline. Antimicrob Agents Chemother 1966;6:371–6.
[62] Rudjito R, Agalave NM, Farinotti AB, Lundbäck P, Szabo-Pardi TA, Price TJ, Harris HE, Burton MD, Svensson CI. Sex- and cell-dependent contribution of peripheral high mobility group box 1 and TLR4 in arthritis-induced pain. PAIN 2021;162:459–70.
[63] Sadler KE, Langer SN, Menzel AD, Moehring F, Erb AN, Brandow AM, Stucky CL. Gabapentin alleviates chronic spontaneous pain and acute hypoxia-related pain in a mouse model of sickle cell disease. Br J Haematol 2019;187:246–60.
[64] Sadler KE, Lewis TR, Waltz TB, Besharse JC, Stucky CL. Peripheral nerve pathology in sickle cell disease mice. PAIN Rep 2019;4:e765.
[65] Sadler KE, Moehring F, Shiers SI, Laskowski LJ, Mikesell AR, Plautz ZR, Brezinski AN, Mecca CM, Dussor G, Price TJ, McCorvy JD, Stucky CL. Transient receptor potential canonical 5 mediates inflammatory mechanical and spontaneous pain in mice. Sci Transl Med 2021;13: eabd7702.
[66] Sadler KE, Zappia KJ, O'Hara CL, Langer SN, Weyer AD, Hillery CA, Stucky CL. Chemokine (c-c motif) receptor 2 mediates mechanical and cold hypersensitivity in sickle cell disease mice. PAIN 2018;159:1652–63.
[67] Scaffidi P, Misteli T, Bianchi ME. Release of chromatin protein HMGB1 by necrotic cells triggers inflammation. Nature 2002;418:191–5.
[68] Sorge RE, LaCroix-Fralish ML, Tuttle AH, Sotocinal SG, Austin JS, Ritchie J, Chanda ML, Graham AC, Topham L, Beggs S, Salter MW, Mogil JS. Spinal cord toll-like receptor 4 mediates inflammatory and neuropathic hypersensitivity in Male but not female mice. J Neurosci 2011;31:15450–4.
[69] Sorge RE, Mapplebeck JCS, Rosen S, Beggs S, Taves S, Alexander JK, Martin LJ, Austin JS, Sotocinal SG, Chen D, Yang M, Shi XQ, Huang H, Pillon NJ, Bilan PJ, Tu Y, Klip A, Ji RR, Zhang J, Salter MW, Mogil JS. Different immune cells mediate mechanical pain hypersensitivity in male and female mice. Nat Neurosci 2015;18:1081–3.
[70] Thomson AM, McHugh TA, Oron AP, Teply C, Lonberg N, Vilchis Tella VM, Wilner LB, Fuller K, Hagins H, Aboagye RG, Aboye MB, Abu-Gharbieh E, Abu-Zaid A, Addo IY, Ahinkorah BO, Ahmad A, AlRyalat SAS, Amu H, Aravkin AY, Arulappan J, Atout MMW, Badiye AD, Bagherieh S, Banach M, Banakar M, Bardhan M, Barrow A, Bedane DA, Bensenor IM, Bhagavathula AS, Bhardwaj P, Bhardwaj PV, Bhat AN, Bhutta ZA, Bilalaga MM, Bishai JD, Bitaraf S, Boloor A, Butt MH, Chattu VK, Chu DT, Dadras O, Dai X, Danaei B, Dang AK, Demisse FW, Dhimal M, Diaz D, Djalalinia S, Dongarwar D, Elhadi M, Elmonem MA, Esezobor CI, Etaee F, Eyawo O, Fagbamigbe AF, Fatehizadeh A, Force LM, Gardner WM, Ghaffari K, Gill PS, Golechha M, Goleij P, Gupta VK, Hasani H, Hassan TS, Hassen MB, Ibitoye SE, Ikiroma AI, Iwu CCD, James PB, Jayaram S, Jebai R, Jha RP, Joseph N, Kalantar F, Kandel H, Karaye IM, Kassahun WD, Khan IA, Khanmohammadi S, Kisa A, Kompani F, Krishan K, Landires I, Lim SS, Mahajan PB, Mahjoub S, Majeed A, Marasini BP, Meresa HA, Mestrovic T, Minhas S, Misganaw A, Mokdad AH, Monasta L, Mustafa G, Nair TS, Narasimha Swamy S, Nassereldine H, Natto ZS, Naveed M, Nayak BP, Noubiap JJ, Noyes T, Nri-Ezedi CA, Nwatah VE, Nzoputam CI, Nzoputam OJ, Okonji OC, Onikan AO, Owolabi MO, Patel J, Pati S, Pawar S, Petcu IR, Piel FB, Qattea I, Rahimi M, Rahman M, Rawaf S, Redwan EMM, Rezaei N, Saddik B, Saeed U, Saheb Sharif-Askari F, Samy AM, Schumacher AE, Shaker E, Shetty A, Sibhat MM, Singh JA, Suleman M, Sunuwar DR, Szeto MD, Tamuzi JJL, Tat NY, Taye BT, Temsah MH, Umair M, Valadan Tahbaz S, Wang C, Wickramasinghe ND, Yigit A, Yigit V, Yunusa I, Zaman BA, Zangiabadian M, Zheng P, Hay SI, Naghavi M, Murray CJL, Kassebaum NJ. Global, regional, and national prevalence and mortality burden of sickle cell disease, 2000–2021: a systematic analysis from the Global Burden of Disease Study 2021. Lancet Haematol 2023;10:e585–99.
[71] Valverde Y, Benson B, Gupta M, Gupta K. Spinal glial activation and oxidative stress are alleviated by treatment with curcumin or coenzyme Q in sickle mice. Haematologica 2016;101:e44–7.
[72] Vercellotti GM, Zhang P, Nguyen J, Abdulla F, Chen C, Nguyen P, Nowotny C, Steer CJ, Smith A, Belcher JD. Hepatic overexpression of hemopexin inhibits inflammation and vascular stasis in murine models of sickle cell disease. Mol Med 2016;22:437–51.
[73] Vingert B, Tamagne M, Desmarets M, Pakdaman S, Elayeb R, Habibi A, Bernaudin F, Galacteros F, Bierling P, Noizat-Pirenne F, Cohen J. Partial dysfunction of Treg activation in sickle cell disease. Am J Hematol 2014; 89:261–6.
[74] Vissa M, Larkin SK, Vichinsky EP, Kuypers FA, Soupene E. Assessment of total and unbound cell-free heme in plasma of patients with sickle cell disease. Exp Biol Med 2023;248:897–907.
[75] Wang W, Liu WZ, Wang ZL, Duan DX, Wang XY, Liu SJ, Wang ZJ, Xing GG, Xing Y. Spinal microglial activation promotes perioperative social defeat stress-induced prolonged postoperative pain in a sex-dependent manner. Brain Behav Immun 2022;100:88–104.
[76] Wu LC, Sun CW, Ryan TM, Pawlik KM, Ren J, Townes TM. Correction of sickle cell disease by homologous recombination in embryonic stem cells. Blood 2006;108:1183–8.
[77] Xu H, Wandersee NJ, Guo YH, Jones DW, Holzhauer SL, Hanson MS, Machogu E, Brousseau DC, Hogg N, Densmore JC, Kaul S, Hillery CA, Pritchard KA. Sickle cell disease increases high mobility group box 1: a novel mechanism of inflammation. Blood 2014;124:3978–81.
[78] Yang H, Hreggvidsdottir HS, Palmblad K, Wang H, Ochani M, Li J, Lu B, Chavan S, Rosas-Ballina M, Al-Abed Y, Akira S, Bierhaus A, Erlandsson-Harris H, Andersson U, Tracey KJ. A critical cysteine is required for HMGB1 binding to toll-like receptor 4 and activation of macrophage cytokine release. Proc Natl Acad Sci U S A 2010;107:11942–7.
[79] Yang H, Zeng Q, Silverman HA, Gunasekaran M, George SJ, Devarajan A, Addorisio ME, Li J, Tsaava T, Shah V, Billiar TR, Wang H, Brines M, Andersson U, Pavlov VA, Chang EH, Chavan SS, Tracey KJ. HMGB1 released from nociceptors mediates inflammation. Proc Natl Acad Sci U S A 2021;118:e2102034118.
[80] Yang L, Zheng C, Xia YF, Dai Y, Wei ZF. 3, 3'-diindolylmethane enhances macrophage efferocytosis and subsequently relieves visceral pain via the AhR/Nrf2/Arg-1-mediated arginine metabolism pathway. Phytomedicine 2023;116:154874.
[81] Yang YW, Chen MK, Yang BY, Huang XJ, Zhang XR, He LQ, Zhang J, Hua ZC. Use of 16S rRNA gene-targeted group-specific primers for real-time PCR analysis of predominant bacteria in mouse feces. Appl Environ Microbiol 2015;81:6749–56.
[82] Zappia KJ, Garrison SR, Hillery CA, Stucky CL. Cold hypersensitivity increases with age in mice with sickle cell disease. PAIN 2014;155: 2476–85.